ELSEVIER

Microporous Materials 10 (1997) 111–121

MICROPOROUS
MATERIALS

Effect of delayed neutralization on the synthesis of mesoporous MCM-41 molecular sieves

Hong-Ping Lin, Soofin Cheng, Chung-Yuan Mou *

Department of Chemistry, National Taiwan University, Taipei, Taiwan 106, PR China

Received 10 July 1996; accepted 1 December 1996

Abstract

We present a detailed study on the preparation of highly-ordered MCM-41 molecular sieves based on a new delayed neutralization process. Products synthesized from cationic surfactants with different carbon chain lengths (alkyltrimethylammonium salt), counterions and head groups gave almost constant wall thickness (about 1.7 nm), small lattice contraction after calcination, and sharp pore size distribution. However, the structural order decreased with the decrease of the carbon chain length. Adding a proper amount of alcohols as cosurfactants would improve the XRD patterns of the surfactants with carbon chain lengths less than 14. A head group of larger size would shrink the pore size and damage somewhat the structural order of MCM-41 materials. The rate of acidification and the source of the acid did not have much effect on the XRD patterns of MCM-41, but would affect its morphology. The formation process and the nature of the MCM-41 product based on octadecyltrimethylammonium bromide (C_{18}TMAB) are dependent on the synthetic temperature.

Keywords: Delayed neutralization; MCM-41; Mesostructure; Molecular sieves

1. Introduction

Recently, researchers at Mobil R&D Corp. have discovered a new family of silicate and aluminosilicate mesoporous molecular sieves designed as M41S [1,2]. One member of this family, MCM-41, possessing a hexagonal arrangement of uniformly sized mesopore with adjustable pore size (1.5–10.0 nm), high surface area, high hydrocarbon sorption capacities and high thermal stability, has attracted the attention of many scientists, because it covers a new range of potential applications as catalysts, supporters or advanced materials. Up to now, there have been many reports on the synthetic method and formation mechanism of the mesoporous MCM-41 materials [3–7].

The MCM-41 materials were formed from the combination of the silica polyanionic species with the micelles of surfactant. The micellar structure of a surfactant has great influence on the structure of the MCM-41 products. Beck et al. [8] reported that the XRD patterns of the MCM-41 materials became less well-defined with surfactants of shorter carbon chain length. This is in parallel with the micellar behavior of the surfactant; surfactants with longer chain lengths can form larger micelles more easily. These then have greater affinity to the

* Corresponding author. Fax: 886 2 3636359;
e-mail: cymou@ccms.ntu.edu.tw

PII S0927-6513(96)00125-3

silica polyanionic species and induce the formation of highly ordered MCM-41 structure. Due to the complex nature of the gel mixture and formation mechanism of the MCM-41, the shape of the XRD pattern, the pore size distribution, the lattice contraction after calcination and the wall thickness of MCM-41 material were reported to be dependent on the synthetic condition and the gel precursors [9–13]. There are still many factors which need to be explored in order to further understand the formation mechanism and improve the structure of the MCM-41 materials. In this paper, we report the effect of surfactant chain length, head group, counterion, temperature and cosurfactant on the formation of MCM-41 materials.

It has been shown by Stucky and co-workers [10] that the kinetic process of formation of MCM-41 can be divided into three stages with decreasing rate: cation–anion association, mesostructure formation, and silica condensation. Fyfe and Fu [13] have exploited this separation of stages by employing HCl vapor to affect structural transformation. Our approach is to start the synthesis process using silicates under high pH (~13) conditions, such that mesostructure can be formed first, and then we observe a structural transformation by a delayed neutralization, e.g., delayed silica condensation. We have found that this process leads to a better synthesis procedure at room temperature [14]. High crystallinity and less lattice constriction after calcination were observed in the resulting MCM-41 products.

In the present work, we used the delayed neutralization method in this new process and obtained MCM-41 materials of different morphology. The effects of the variation of the surfactant and experimental factors on the formation of the MCM-41 materials was studied. Factors under examination include the chain length, counterion, head group size of the surfactant and the addition of cosurfactant (such as butanol). Moreover, the rate of acidification, the source of the acid and temperature for synthesis were found to exert influence on the pore size, the structural order and the morphology of the MCM-41 material. Summarizing these effects, we will discuss the observed variation in trends in terms of packing considerations in the formation of rod-like micelles and hexagonal phase.

2. Experiment

2.1. Materials

The silica source was sodium silicate (27% SiO_2, 14% NaOH) from Aldrich. The quaternary ammonium surfactant compounds $C_nH_{2n+1}(CH_3)_3NX$ or $C_nH_{2n+1}NC_5H_5X$, X=Cl, Br or NO_3, were obtained from Aldrich, Merck or Tokyo Chemical Industry without further purification. The source of aluminum was sodium aluminate from Riede-de Haën. Sulfuric acid, hydrochloric acid, acetic acid, nitric acid, phosphoric acid and perchloric acid were obtained from Merck or Janssen Chimica.

2.2. Synthetic procedure

To prepare pure-silica MCM-41 materials, sodium silicate was added to a clear aqueous solution of the surfactant under stirring and a gel mixture was formed. After stirring for about 10 min at room temperature or at 50°C, a proper amount of 1.10 M sulfuric acid or other acids was added into the gel mixture and the pH value was adjusted to about 9.5–10. Here, two different acidification rates were used. One is to add the entire acid to the gel mixture at once — 'immediate acidification'; the other is to add the acid drop by drop over about 30 min with a pipette — 'gradual acidification'. The molar ratio of the resultant gel composition is 1 SiO_2:0.48 surfactant:0.39 Na_2O:0.29 H_2SO_4:50–100 H_2O. Then, the mixture was stirred for 20 min and loaded into an autoclave and statically heated at 100°C for 48 h. The resulting solid products were recovered by filtration, washed with deionized water and dried in air at room temperature or 100°C. To remove the organic species occluded in the pores of MCM-41, the as-synthesized samples were calcined in air at 560°C for 6 h (heated from room temperature to 560°C with a heating rate of 1.5°C min^{-1}).

The aluminosilicate MCM-41 was synthesized with the same process mentioned above except

that a suitable amount of sodium aluminate was added into the solution of surfactant in the first step.

2.3. Characterization

X-ray powder diffraction (XRD) data were collected on a Scintag X1 diffractometer using Cu Kα radiation ($\lambda = 0.154$ nm). N_2 adsorption–desorption isotherms were obtained at 77 K on a Micrometric ASAP 2000 apparatus. The sample was outgassed at 300°C for about 6 h in 10^{-3} Torr prior to adsorption. The pore size distribution curves were obtained from the analysis of the desorption portion of the isotherms using the BJH (Barrett-Joyner-Halenda) method. The transmission electron micrographs (TEM) were taken on a Hitachi H-7100 operated at 100 keV. Scanning electron microscopy (SEM) was performed on a Hitachi S-2400 using an accelerating voltage of 20 keV. The solid state ^{27}Al MAS NMR experiments were performed at room temperature on a Bruker MSL 500 NMR with a magnetic field of 11 T.

3. Results

3.1. Acidification rate

We have shown in our previous report that the acidification rate is an important factor to prepare the MCM-41 materials of highly-ordered arrangement and special morphology in a delayed neutralization method. By careful control of the rate of acidification, a new tubules-within-a-tubule order can be obtained [15].

First, we explored the effect of acidification rate on the MCM-41 products synthesized with different surfactants. Fig. 1(A) shows that the product of the C_{16}TMAB-aluminosilicate system synthesized with the gradual acidification process has a hollow tubular structure with coaxial cylindrical nanometer channels of MCM-41 constituting the wall of the tubules as reported previously in Ref. [15]. However, the products from immediate acidification only have microparticle morphology (Fig. 1(B)). Similar phenomena were observed for the MCM-41 products prepared with surfactants of carbon chain length longer than 12. The XRD patterns and pore sizes of all these products are nevertheless independent of the neutralization rate. However, when a surfactant with carbon chain length shorter or equal than 12 was used, the immediate acidification process would result in the products with more ordered arrangement of hexagonal arrays than those obtained by gradual acidification. For example, the product of the C_{12}TMAB-silicate system has only two broad

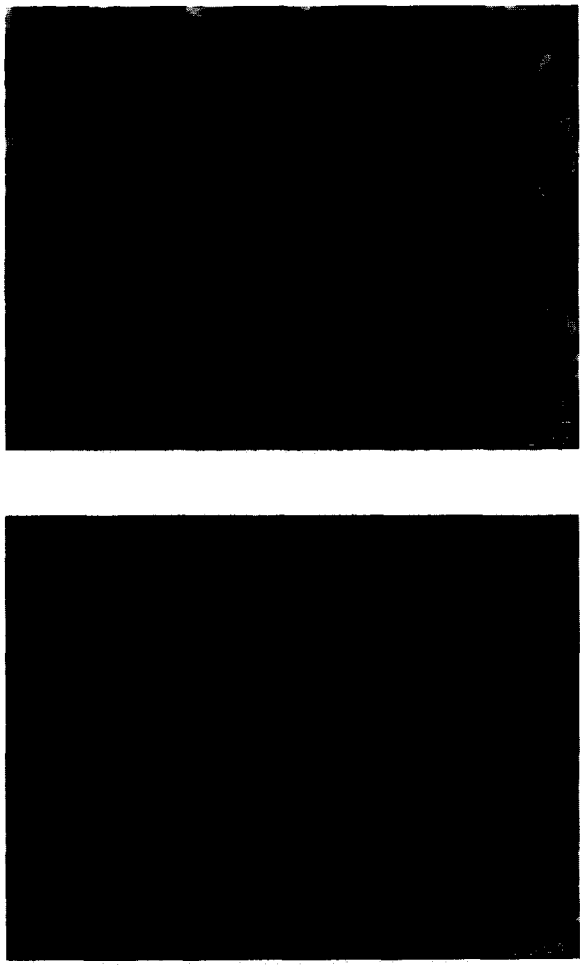

Fig. 1. Scanning electron micrograph of the as-synthesized MCM-41 materials prepared from the C_{16}TMAB-alunimosilicate system with Si/Al=37 using different acidification rates. (A) Gradual acidfication; (B) immediate acidification.

XRD peaks under the conditions of gradual acidification, but four sharper peaks are observed from immediate acidification (Fig. 2(A,B)).

We also synthesized the MCM-41 materials of all these surfactants by the method previously published by others [1,2,9], where the silicate and acid were combined before the addition into the surfactant solution. It is found that the morphologies of these MCM-41 products were all in microparticles, as reported in the literature, and the XRD patterns of the products prepared from the surfactants of the carbon chain length shorter than 12 consist of only two broad peaks (Fig. 2(C)). Thus, the delayed neutralization process is a better method to synthesize highly-ordered MCM-41 materials, and a hierarchical structure of tubules-within a-tubule could be obtained. Using the delayed neutralization method, the gradual acidification process is suitable for the preparation of a hierarchical morphology of MCM-41 materials with surfactants of carbon chain length longer than 12, and the immediate acidification process would give particulate morphology while improving the structural order of the products.

3.2. Chain length

Fig. 3 shows the X-ray diffraction (XRD) patterns of the calcined pure silica MCM-41 products synthesized from alkyltrimethylammonium salts (C_nTMAX, X=B for Br or Cl for Cl, n=8–18) with carbon chain number varying from 8 to 18 (A–F in Fig. 3) by using immediate acidification process. The XRD patterns show that the d_{100} value increases and the peaks become sharper as the carbon chain length increases. Moreover, for MCM-41 materials prepared with C_{16}TMACl and

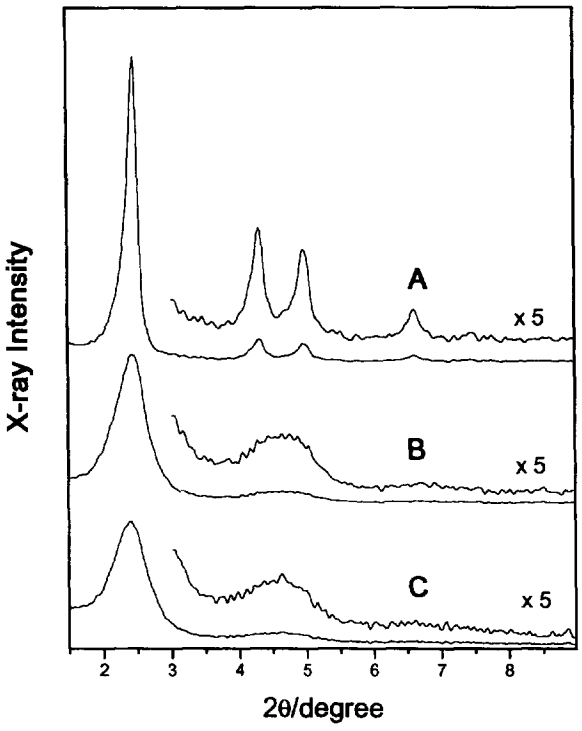

Fig. 2. X-ray powder diffraction patterns of the as-synthesized products prepared from the C_{12}TMAB-silicate system using different synthetic processes. (A) Delayed neutralization with immediate acidification; (B) delayed neutralization with gradual acidification; (C) without delayed neutralization.

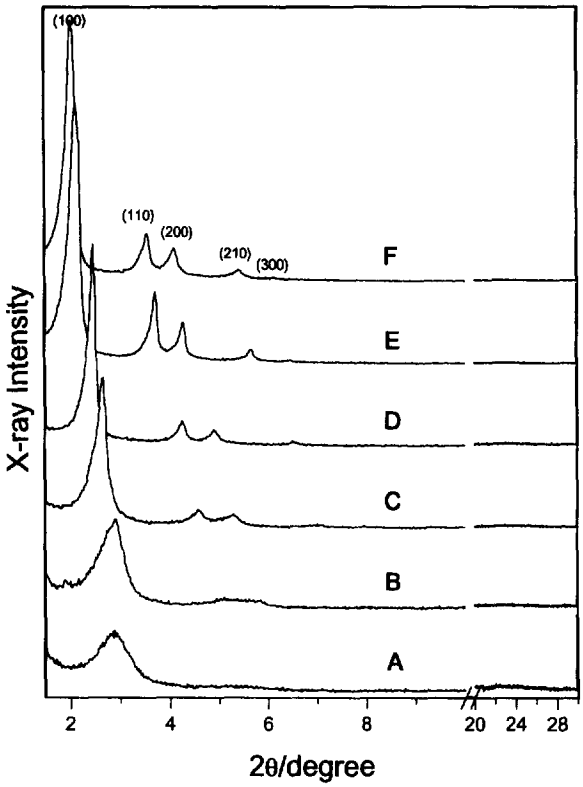

Fig. 3. X-ray powder diffraction patterns of calcined products prepared using different surfactants. (A) C_8TMAB; (B) C_{10}TMAB; (C) C_{12}TMAB; (D) C_{14}TMAB; (E) C_{16}TMACl; (F) C_{18}TMACl.

C_{18}TMACl surfactants, there appear five XRD peaks, one more than the four peaks generally reported previously [2–9]. This additional d_{300} peak indicates that the MCM-41 solids prepared by this new method are more ordered than those prepared by the previously reported methods. The delayed neutralization process leaves more time for the micelles and silica polyanionic species to assemble into a more regular pattern. Nevertheless, the structural order of the MCM-41 products decreases when the surfactants of shorter carbon chain length were used. This is accounted for by the weakening of interactions between the silica polyanionic species and the surfactants with shorter carbon chain length, similar behavior also being observed in surfactant–polyelectrolyte systems [16,17]. Besides, the XRD baselines of all samples prepared by this process are almost flat at $2\theta = 20$–$30°$, implying that few microparticles of amorphous silica are formed using this method. In other words, the delayed neutralization process offers a convenient procedure to produce highly-ordered MCM-41 mesoporous materials with low amorphous silica impurity.

The N_2 adsorption-desorption isotherms of the calcined samples prepared with C_{18}TMACl, C_{14}TMAB and C_{10}TMAB are shown in Fig. 4. All of these samples have BET surface area greater than 1000 $m^2 g^{-1}$. For each curve, there is a sharp increase in adsorbed volume at a certain relative pressure p/p_0, which corresponds to the capillary condensation in the mesopores of the materials. The pore size distributions calculated from N_2 desorption curves are quite narrow, indicating that this method would produce MCM-41 materials of uniformly-sized mesopores. The C_{18}TMACl sample has a pore size distribution centered around 3.15 nm, with a half-width of about 0.19 nm; the C_{14}TMAB sample gives the corresponding values of 2.56 and 0.18 nm, and those of the C_{10}TMAB sample are 2.17 and 0.23 nm. Furthermore, the *t*-plots of these MCM-41 materials were examined. All of these samples have near zero intercepts, which indicates that the products have no microporous structures [18,19].

We also synthesized the MCM-41 solids with many other surfactants. Table 1 compares the pore size, *d*-spacing and the wall thickness of the solids prepared with different carbon chain lengths, counterions and head groups of the surfactants. The approximate pore size was obtained from the N_2 sorption isotherm and the repeat distance (a_0) was calculated by X-ray diffraction data with the equation $a_0 = 2d_{100}/\sqrt{3}$. The wall thickness was determined by the difference between the repeat distance (a_0) and pore size [2,4,9,20]. All of these MCM-41 materials have a BET surface area of around 1000 $m^2 g^{-1}$. Although the pore size and *d*-spacing increase with the carbon chain length of the surfactant, the products prepared from surfactants with the same carbon chain length but different counterion and head group have almost the same pore size and *d*-spacing. This indicates that the counterions bound to the interface of the micelle of the surfactant are replaced by the silica polyanionic species during the synthetic process. The head group is relatively small compared with the carbon chain, so that the pore size is mainly dependent on the carbon chain length. The wall thicknesses of the MCM-41 materials synthesized by this method are in the small range of

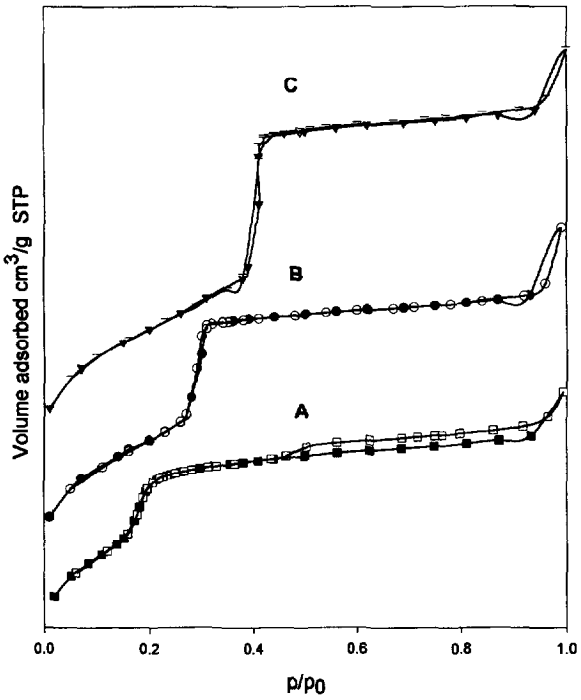

Fig. 4. N_2 adsorption-desorption isotherms of the calcined MCM-41 materials. (A) C_{10}TMAB; (B) C_{14}TMAB; (C) C_{18}TMAB.

Table 1
Effect of surfactant chain length, counterion, head group on MCM-41 pore size, XRD d_{100} value, hexagonal unit cell parameter a_0 and the wall thickness

Surfactant	XRD d_{100} (d-spacing, nm)	a_0^a (nm)	N_2 pore size (nm)	Wall thickness (nm)
$C_nH_{2n+1}(CH_3)_3NX$[b]				
C_{18}TMAB[c]	4.30	4.96	3.23	1.73
C_{18}TMACl	4.28	4.94	3.18	1.76
C_{16}TMAB	3.96	4.57	2.87	1.70
C_{16}TMACl	3.98	4.59	2.87	1.72
C_{16}TMAN	4.00	4.61	2.86	1.75
C_{14}TMAB	3.61	4.17	2.56	1.61
C_{12}TMAB	3.31	3.82	2.21	1.61
C_{10}TMAB	3.15	3.64	1.92	1.72
C_8TMAB	2.90	3.35	1.67	1.68
$C_nH_{2n+1}NC_5H_5X$[d]				
C_{16}PyB	3.95	4.56	2.72	1.84
C_{16}PyCl	4.01	4.63	2.72	1.91
C_{12}PyCl	3.32	3.83	2.23	1.65

[a] $a_0 = 2d_{100}/\sqrt{3}$ as distance of nearest pore centers. [b] Alkyltrimethylammonium halide. [c] Synthesized at 50°C. [d] Alkylpyridinium halide.

1.60–1.91 nm. In the C_nTMABX system, the wall thickness is around 1.70 nm, not dependent on the nature of the surfactant. The uniformly thicker walls make the MCM-41 materials synthesized by this method more rigid. They shrink less (about 0.12–0.22 nm) after calcination and have a sharper pore size distribution (about 0.14–0.23 nm) than those previously reported [2,9,20].

The transmission electron micrographs (TEM) of the as-synthesized samples of C_{16}TMAB and C_{10}TMAB illustrate the regular hexagonal array of mesoporous channels (Fig. 5(A,B)). The repeating distances between pores are about 4.3 and 3.5 nm for C_{16}TMAB and C_{10}TMAB, in excellent agreement with those obtained from XRD patterns.

3.3. Cosurfactant: BuOH

Because the surfactant with the shorter carbon chain length has less affinity to the silica polyanionic species, the products synthesized from C_8TMAB, C_{10}TMAB and C_{12}PyCl-silicate systems have less well-defined XRD patterns. Based on the principle of micelle formation, adding a proper amount of cosurfactant, such as butanol (BuOH) or hexanol (HeOH), can elongate the length of micelle to favor the interaction between micelles and silica polyanionic species [21,22]. Hence, some cosurfactants were added to the synthetic composition of C_8TMAB, C_{10}TMAB and C_{12}PyCl-silicate systems and their effects on structural order were examined. Fig. 6 shows that by adding BuOH in a suitable BuOH/surfactant range, the two diffuse XRD peaks of C_{10}TMAB products can change into three or four sharp peaks (Fig. 6). This is similar to that of C_{12}PyCl. But the addition of BuOH has no effect on the samples prepared from the surfactant with even shorter carbon chain length (C_8TMAB). It is believed that the chain length of C_8TMAB is too short to form an energetically favorable liquid crystal structure [23]. We concluded that adding short chain alcohols (BuOH) as cosurfactants can improve the formation of the hexagonal structure of MCM-41 with surfactants in a marginal case such as C_{10}TMAB.

3.4. Head group

The effect of the head group size of the surfactant on the synthesis of MCM-41 materials was also examined. Fig. 7 shows the XRD pattern of the products from C_{16}TMAB: cetyldimethylethylammonium bromide (C_{16}DMEAB) has four sharp

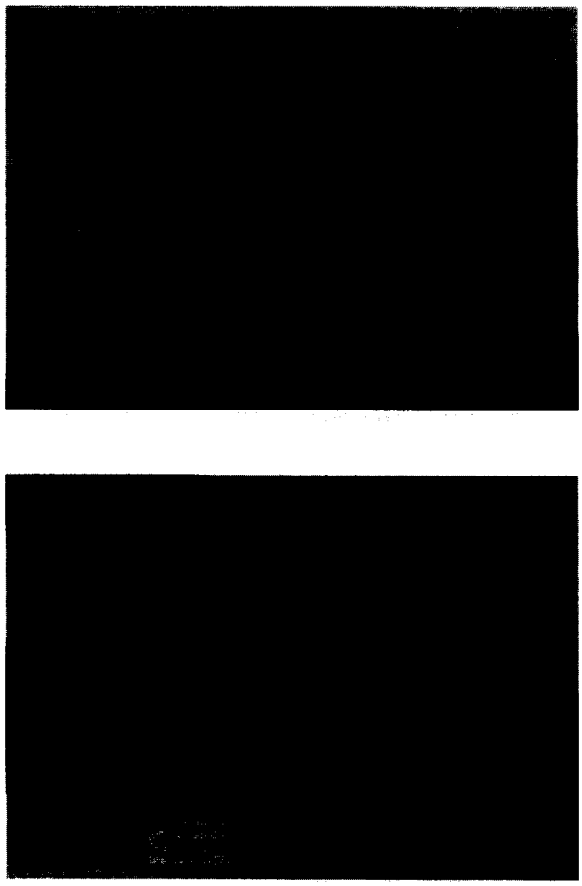

Fig. 5. Transmission electron micrographs of the as-synthesized MCM-41. (A) C_{16}TMAB; (B) C_{10}TMAB.

peaks and $d_{100}=4.0$ nm; while that from cetylbenzyldimethylammonium bromide (C_{16}BDMAB) has two broad XRD peaks and a smaller *d*-spacing of 3.6 nm. The less ordered arrangement and smaller *d*-spacing of the latter suggest that the benzyl group is probably interacting with the cetyl group ($C_{16}H_{33}$). As a result, the effective chain length of the surfactant shrinks, which leads to a smaller pore diameter of the MCM-41 product. Moreover, the head group of C_{16}BDMAB has more steric hindrance than the other two surfactants; this might lead to poor hexagonal packing and result in more diffuse XRD patterns.

3.5. The nature of the acid

A variety of acids other than H_2SO_4, such as H_3PO_4, $HClO_4$, HNO_3, HCl and CH_3COOH,

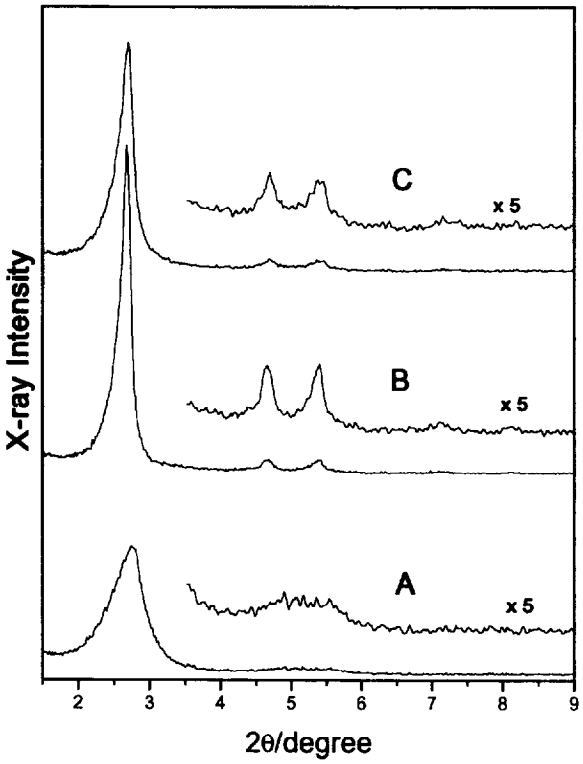

Fig. 6. X-ray powder diffraction patterns of the as-synthesized products prepared from different BuOH/C_{10}TMAB ratios using immediate acidification. (A) BuOH/C_{10}TMAB=0; (B) BuOH/C_{10}TMAB=0.75; (C) BuOH/C_{10}TMAB=1.08.

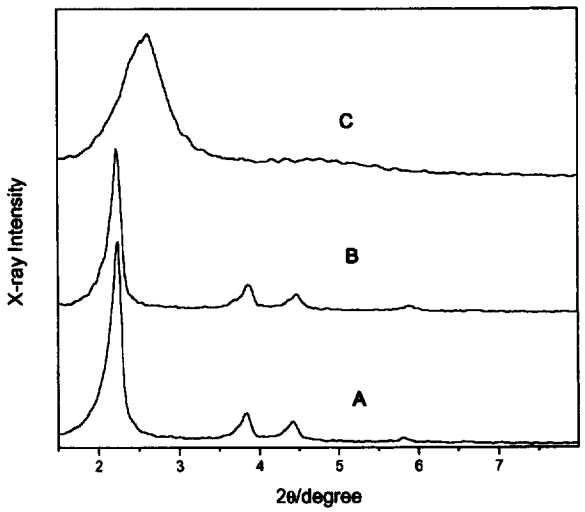

Fig. 7. X-ray powder diffraction patterns of the calcined products prepared using surfactants with different head group sizes. (A) C_{16}TMAB; (B) C_{16}DMEAB; (C) C_{16}BDMAB.

were used to synthesize the MCM-41 materials. All these acids, except HNO_3, result in products with well-defined XRD patterns, sharp pore size distribution and the same morphology as that synthesized from H_2SO_4. But when HNO_3 was used for adjusting the pH value of the mixtures containing surfactants with a carbon chain length longer that 14, a highly viscous gel was obtained, in contrast to those obtained with other acids. The XRD pattern and pore size distribution of the product synthesized from HNO_3 is similar to those from other acids, but the morphology is very different. For instance, in the C_{16}TMACl-silicate system, the products prepared from other acids have the hollow tubular structure (Fig. 8(A)), while the product synthesized from HNO_3 is in microparticle form (Fig. 8(B)). This is probably because the nitrate ion (NO_3^-) has the largest binding strength to the cationic micelles among these acids which forms a very viscous intermediate, inhibiting the production of microtubule [24]. Therefore HNO_3 is not a suitable acid to produce MCM-41 materials with tubular hierarchical morphology.

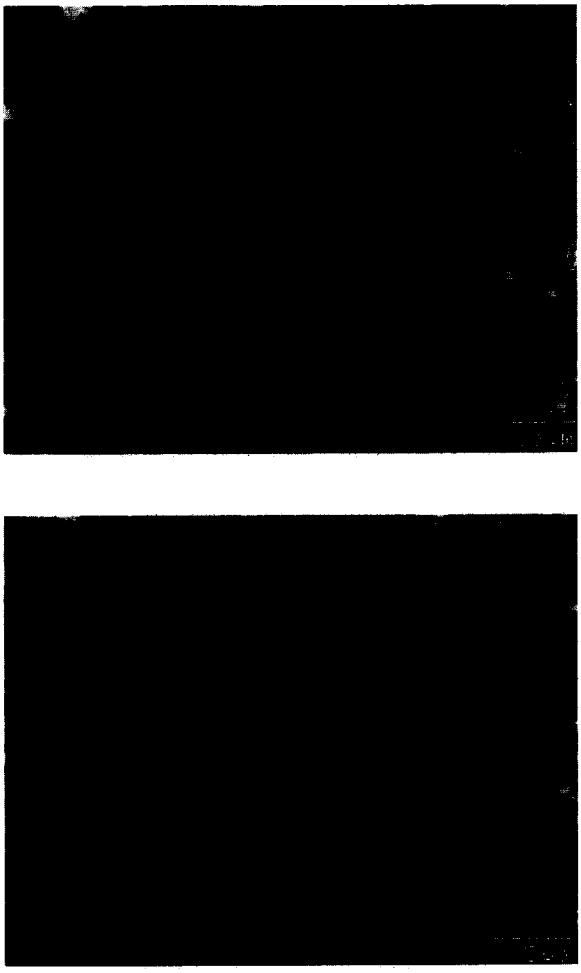

Fig. 8. Scanning electron micrograph of the calcined MCM-41 materials prepared from the C_{16}TMACl-silicate system with different acids using gradual acidification. (A) CH_3COOH; (B) HNO_3.

3.6. Temperature effect for C_{18}TMAB

The MCM-41 materials of all the surfactants synthesized at room temperature have well-defined hexagonal XRD patterns, but the product of C_{18}TMAB is a special case. We compared the XRD pattern of the calcined C_{18}TMAB product whose gel mixture was prepared at room temperature with that prepared at 50°C (Fig. 9(A,B)). The latter has four sharp peaks and a *d*-spacing of about 4.22 nm, but the former has just two diffuse peaks and a *d*-spacing of 4.0 nm. In order to understand the effect of temperature on the C_{18}TMAB product, the as-synthesized solids, after complete addition of the acid at room temperature and 50°C, were examined. A lamellar mesophase was formed under room temperature conditions, but a hexagonal pattern of MCM-41 was obtained at 50°C (Fig. 9(C,D)). These results showed that at room temperature the C_{18}TMAB-silicate system would first form a lamellar mesophase solid, then transform, during hydrothermal reaction, to the final hexagonal mesoporous MCM-41 product. This formation process is similar to that from kanemite–surfactant composition [25]. In the high temperature case (50°C), the hexagonal structure was formed after neutralization, which then led to a more well-defined structure during the hydrothermal reaction. This formation mechanism is parallel to that of the C_{16}TMAB-silicate system at room temperature proposed by Chen et al. [26]. This unique character of C_{18}TMAB is because its long carbon chain tends to form a lamellar phase at room temperature. Hence, the formation mechanism and the structure of the MCM-41 prepared

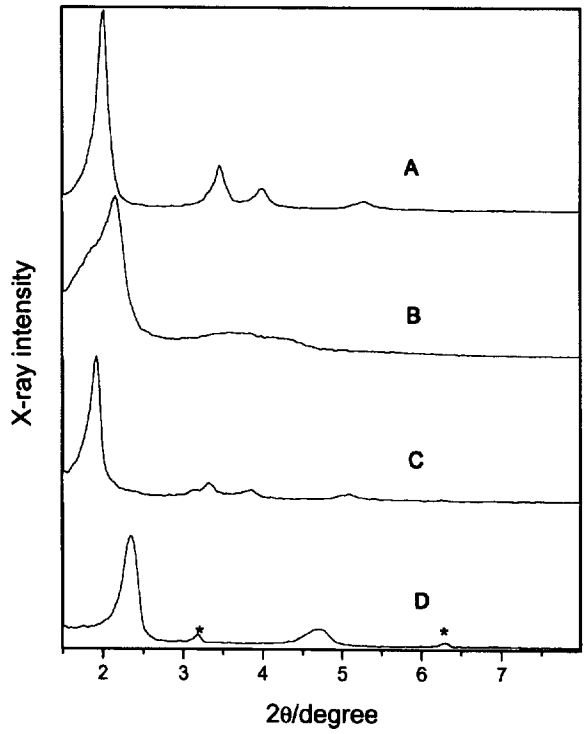

Fig. 9. X-ray powder diffraction patterns of the calcined products of the C_{18}TMAB-silicate system and the as-synthesized solids prepared after complete addition of the acid at different temperatures. (A) calcined product prepared at 50°C; (B) calcined product prepared at room temperature; (C) the as-synthesized solid prepared at 50°C; (D) the as-synthesized solid prepared at room temperature. *Indicates the XRD peaks of the unremoved C_{18}TMAB particles.

from C_{18}TMAB-silicate system would greatly depend on the synthetic temperature.

This synthesis procedure is also suitable for the formation of aluminosilicate MCM-41. As the Si/Al ratio decreases, the XRD patterns become less well-defined and the *d*-spacing value increases. In other words, the incorporation of aluminum into the framework of MCM-41 decreases the order of the mesoporous channels but increases the pore size; this is consistent with the process reported in the literature [27,28]. The ^{27}Al MAS NMR spectra of the products with different Si/Al ratios show that there is only one peak at about 50 ppm in all samples, indicating that the aluminum atoms are in the tetrahedral sites and are likely incorporated in the framework of MCM-41.

4. Discussion

Finally, we present some theoretical considerations for explaining the many observations in this work. Although the mesostructures are formed most probably through a cooperative condensation of surfactant and silicate [10,29], we can divide our theoretical considerations roughly into two parts: the formation of rod-like micelles and the condensation of hexagonal phase.

First, we discuss the relation between the micellar structure and the nature of the MCM-41 product obtained. The form that micelles can take can be explained by simple packing considerations [30]. The organization of surfactant depends on the volume (V_H), length (l_c) occupied by the hydrophobic group and on the effective surface area a_0 of the hydrophilic groups of the surfactant. According to packing requirements, a parameter $p = V_H/l_c a_0$ determines the shape of the micelles. When the value of p is in the region of 0 to 1/3, the micelles of the surfactant are spherical; $p = 1/3$ to 1/2 for cylindrical micelles, and $p = 1/2$ to 1 for lamellar phase. Within the cylindrical micelle range, a higher p value leads to a longer micelle. Such very simple predictions have been confirmed for many surfactant systems: micelles, microemulsion and lamellar phases [31].

At present, we understand little of the formation of the hexagonal phase of rod-like micelles. However, recent theoretical work on the hexagonal phase [32] indicates that its stability depends on the intrinsic rigidity of the micelles and their sizes. Increasing the micellar flexibility favors the hexagonal phase relative to the nematic phase. Long rods favor the hexagonal phase as the entropy gained in randomizing becomes less. With these qualitative ideas, we try to explain the various observations in Section 3.

Let us examine the chain length effect first. Given the same composition in varying surfactant chain length (Section 3.1), the effective surface area a_0 is about the same for C_nTMAX. Thus, the variation in the p parameter comes from the change in molecular volume (V_H) and length (l_c). By using the empirical relations [33]

$$V_H\ (\text{Å}^3) = 27.4 + 26.9n \quad (1)$$

and

$$l_c\ (\text{Å}) = 1.5 + 1.265n, \quad (2)$$

one can see that p is an increasing function of n, the number of carbon atoms in the chain. Thus, accordingly, a longer hydrocarbon group in the surfactant would favor a longer micelle, which is empirically true. And a longer rod would lead to more rigid and ordered packing in the hexagonal phase. Therefore, we observed more well-defined hexagonal structure in MCM-41 as chain length increases, which is shown in Fig. 3.

The addition of butanol to the surfactant/silicate mixture would lead to longer micelles, as observed in a C_{16}TMAB+salt system (J.W. Lu, C.J. Lee and C.Y. Mou, unpublished data) in a dynamic light scattering study. This is due to favored entropy of mixing of BuOH in longer micelles. Since longer rods stabilize the hexagonal phase, we therefore observe that BuOH can improve the hexagonal structure for the case of C_{10}TMAB-made MCM-41.

Larger hydrophobic head group would increase the chain surface area a_0 and lead to shorter rod micelles (smaller p), which in turn result in less ordered hexagonal packing. This is indeed observed in the case of C_{16}BDMAB.

In this work, we have used two different counterions Br^- and Cl^- in the starting surfactants. As long as carbon chain length is fixed, they have very little effect on pore size and lattice d-spacing. This shows that oligosilicates are the mesostructure-directing agents. Indeed, it has been shown that MCM-41 can be synthesized with a surfactant concentration as low as the critical micelle concentration [34]. The strong electrostatic interaction between cationic surfactant and silicate anions is the main determining factor in structure formation. Before acidification, micelles of C_nTMAB and C_nTMACl are very different. The former are long rod-like micelles and the latter are spherical micelles. This is due to stronger micellar dissociation of Cl^- versus Br^-. After acidification, multidentate oligosilicate (highly charged) would replace both Cl^- and Br^- and form the same hexagonal structure. As the anion Y^- of the added acid HY can no longer compete, it does not have any influence on structure (except for morphology).

The constant wall thickness of roughly 1.7 nm, shown in Table 1, is interesting. Previously, researchers have obtained different wall thicknesses, from 0.5 up to 1.7 nm, depending on alkalinity [4]. The larger pore distance comes with lower alkalinity. Our wall thickness of 1.7 nm seems to be the upper bound. This is because, in the delayed neutralization process, we can get to as low a pH value as 9.5 without the formation of amorphous silica. The limiting constant wall thickness in Table 1 seems to indicate that there is a maximum limit to the rod-to-rod distance for the stability of the hexagonal phase. There seem to be a Lindemann-like criterion for the 'melting' of the hexagonal phase. A better understanding is needed with regard to stability factors in the hexagonal phase before the constant thickness can be explained.

As for the effect of temperature, we observed an appreciable effect in the case of C_{18}TMAB. A higher temperature would lead to less counterion association and to a larger a_0, and thus a smaller p value. At room temperature, the C_{18}TMAB-silicate system tends to form a lamellar phase, since n is large enough for the hydrophobic effect to dominate. However, at 50°C, the p value of C_{18}TMAB will decrease to less than 1/2 and thus it forms a hexagonal phase instead. Further hydrothermal reaction at 100°C would transform both lamellar and hexagonal phases into hexagonal packing since the condensation reaction is carried out at a high temperature, where only the hexagonal phase is stable.

5. Conclusions

The delayed neutralization process is an excellent method to synthesize highly-ordered MCM-41 with thicker walls and sharper pore size distributions. It also provides us with a way to explore the interaction between the micelles of the surfactants with different carbon chain lengths, counterions or head groups and the silica polyanionic species. From this, we could progressively probe the intermediates of the surfactant-silicate system

in order to completely understand the formation mechanism of MCM-41 and to control the synthetic conditions in order to obtain desirable MCM-41 materials. This process is also suitable for synthesizing biomimetic hierarchical silica assemblies [15] that may help one to understand the complex biomineralization process [35].

Acknowledgment

This research was supported by the Nation Science Council of Taiwan (NSC 85-2113-31-M-002-032 cc).

References

[1] C.T. Kresge, M.E. Leonowicz, W.J. Roth, J.C. Vartuli and J.S. Beck, Nature, 359 (1992) 710.
[2] J.S. Beck, J.C. Vartuli, W.J. Roth, M.E. Leonowicz, C.T. Kresge, K.D. Schmitt, C.T.-W. Chu, D.H. Olson, E.W. Sheppard, S.B. Higgins and J.L. Schlenker, J. Am. Chem. Soc., 114 (1992) 10834.
[3] A. Monnier, F. Schüth, Q. Huo, D. Kumar, D. Margolese, R.S. Maxwell, G.D. Stucky, M. Krishnamurty, P. Petroff, A. Firouzi, M. Janicke and B.F. Chmelka, Science, 261 (1993) 1299.
[4] N. Coustel, F.D. Renzo and F. Fajula, J. Chem. Soc. Chem. Commun., (1994) 967.
[5] A. Sayari, I. Moudrakovski, C. Danumah, C.I. Ratcliffe, J.A. Ripmeester and K.F. Preston J. Phys. Chem., 99 (1995) 16373.
[6] R. Ryoo and J.M. Kim, J. Chem. Soc. Chem. Commun., (1995) 711.
[7] C.F. Cheng, Z. Luan and J. Klinowski, Langmuir, 11 (1995) 2815.
[8] J.S. Beck, J.C. Vartuli, G.J. Kennedy, C.T. Kresge, W.J. Roth and S.E. Schramm, Chem. Mater., 6 (1994) 1816.
[9] C.Y. Chen, H.X. Li and M.E. Davis, Microporous Mater., 2 (1993) 17.
[10] Q. Huo, D.I. Margolese, U. Ciesla, D.G. Demuth, P. Feng, T.E. Gier, P. Sieger, A. Firouzi, B.F. Chmelka, F. Schüth and G.D. Stucky, Chem. Mater., 6 (1994) 1176.
[11] Q. Hou, R. Leon, P.M. Petroff and G.D. Stucky, Science, 268 (1995) 1324.
[12] Q. Hou, D.I. Margolese and G.D. Stucky, Chem. Mater. 8 (1996) 1147.
[13] G.A. Fyfe and G. Fu, J. Am. Chem. Soc., 117 (1995) 9709.
[14] H.P. Lin, S. Cheng and C.Y. Mou, J. Chin. Chem. Soc., 43 (1996) 375.
[15] H.P. Lin and C.Y. Mou, Science, 273 (1996) 765.
[16] K. Thalberg, B. Lindam and G. Karlström, J. Phys. Chem., 94 (1990) 4289.
[17] K. Thalberg and B. Lindam, J. Phys. Chem., 95 (1991) 3370.
[18] P.J. Branton, P.G. Hall and K.S.W. Sing, J. Chem. Soc. Chem. Commun., (1993) 1257.
[19] P.J. Branton, P.G. Hall, K.S.W. Sing, H. Reichert, F. Schüth and K.K. Unger, J. Chem. Soc. Faraday Trans., 90 (1994) 2965.
[20] C.N. Wu, T.S. Tsai, C.N. Liao and K.J. Chao, Microporous Mater., 7 (1996) 173.
[21] S. Candau and R. Zaana, J. Colloid Interface Sci., 84 (1981) 206.
[22] M. Almgren and S. Swarup, J. Colloid Interface Sci., 91 (1983) 256.
[23] G.J. Tiddy, Phys. Rev., 57 (1980) 1.
[24] L. Sepúlveda and J. Cortés, J. Phys. Chem., 89 (1985) 5322.
[25] C.Y. Chen, S.Q. Xiao and M.E. Davis, Microporous Mater., 4 (1995) 1.
[26] C.Y. Chen, S.L. Burkett, H.X. Lin and M.E. Davis, Microporous Mater., 2 (1993) 27.
[27] Z. Luan, H. He, W. Zhou, C.-F. Cheng and J. Klinowski, J. Chem. Soc. Faraday Trans., 91 (1995) 2955.
[28] K.R. Kloetstra, H.W. Zandbergen and H.v. Bekkum, Catal. Lett., 33 (1995) 157.
[29] A. Firouzi, D. Kumar, T. Besier, P. Sieger, Q. Huo, S.A. Walker, J.A. Zasadzinski, C. Glinka, J. Nicol, D. Margolese, G.D. Stucky and B.F. Chmelka, Science, 267 (1995) 1138.
[30] J.N. Israolachvili, D.J. Mitchell and B.W. Ninham, J. Chem. Soc. Faraday Trans., 72(2) (1976) 1525.
[31] D. Langevin, Ann. Rev. Phys. Chem., 43 (1992) 341.
[32] P. Van der Schoot, J. Chem. Phys., 104 (1996) 1130.
[33] C. Tanford, The Hydrophobic Effect, New York, Wiley, 1973.
[34] C.-F. Cheng, Z. Luan and J. Klinowski, Langmuir, 11 (1995) 2815.
[35] S. Mann and G.A. Ozin, Nature, 382 (1996) 313.